JOURNAL OF MATERIALS SCIENCE 30 (1995) 3867–3873

Modelling superplastic deformation of materials with a nonequiaxed microstructure

J. L. WAN, J. L. GU, N. P. CHEN
Materials Science and Engineering Department, Tsinghua University Beijing 100084, People's Republic of China

The superplastic deformation behaviour of a two-dimensional nonequiaxed microstructure is investigated on the basis of the grain-rolling mechanism proposed by Paidar and Takeuchi for an equiaxed microstructure. Analysis shows that not only the deformation geometry but also the dynamics of grain boundary dislocation activity will be altered if grains are elongated rather than equiaxed. Constitutive equations thus derived indicate that the grain aspect ratio can impose a remarkable influence on the superplastic stress–strain rate relationship and such an influence can be quite different if the orientation of the applied stress lies over an angle with respect to the longer axis of the grains. The complexity of modelling the superplastic deformation of engineering materials is also discussed.

1. Introduction

It is well established that the microstructure of a superplastic material should fulfil certain prerequisites—fine-grained, equiaxed, and stable throughout the deformation processes [1–3]. In most cases, achievement of such a microstructure needs the implementation of special manufacturing technology [4]. On the other hand, the possibility of superplastic forming of commercial materials with microstructure that does not fully meet the above-mentioned requirements also attracts both scientific and technological interest because of its economic significance [5–9].

One of the major deviations of commercial material microstructure from the traditional "ideal" one is its elongated grain shape which may be a remainder of insufficient equiaxialization processes [4]. Elongated grains are often arranged along certain spatial directions (e.g. the rolling direction) due to the directional nature of the deformation in the material manufacturing process. When such material is supplied for superplastic forming, anisotropic behaviour occurs [8, 9].

A number of sophisticated theoretical models have been developed to rationalize the phenomenon of superplasticity [10–18]. However, although efforts have been made to extend them into nonequiaxially grained microstructures, the existing developments can only deal with the case where the longer axis of the grains is parallel to the applied tensile stress [19, 20]. One of the reasons could be that in previous models, the basic deformation mechanism—grain boundary sliding (GBS)—and the accommodation processes—diffusion or dislocation creep—were not, or could not be, tightly related to certain grain boundary–stress orientation relationships, which are intrinsically required for the characterization of the deformation behaviours of nonequiaxed microstructures [10–18].

Recently, a model based on grain rolling was proposed by Paidar and Takeuchi [21]. Like most of the former models, the P–T model deals with a microstructure of closely packed hexagonal grains. Grain boundaries were divided into compressive, tensile and sliding facets according to their orientation relationship with the applied stress. Deformation is carried out by shearing of grain layers resulting from the motion of grain boundary dislocations (GBDs) which glide on sliding facets, while accommodation is achieved by climbing of GBDs on the facets with normal stress. Since the orientation dependence of grain boundary behaviours was closely watched in this model, it is quite convenient to extend it into the condition of nonequiaxed microstructures and to investigate the complex anisotropic deformation behaviours that widely exist in the superplastic forming of engineering materials.

2. Model

2.1. Physical basis of the model

The main features of the strain-rate controlling mechanism can be summarized as follows from Paidar and Takeuchi's work:

(1) On the sliding facets, where the shear component of the applied stress plays a major role, gliding GBDs pile up at the grain boundary triple junctions. Each GBD with Burger's vector b_s dissociates into two sessile dislocations $[b_c\sqrt{3}/2, b_c/2]$ and $[b_c\sqrt{3}/2, -b_c/2]$ which enter the other two boundaries. Here $b_c = b_s/\sqrt{3}$.

(2) A pile-up of gliding GBDs can be regarded as a macrodislocation which has a repulsive interaction with the GBDs climbing along the tensile or compressive boundaries. The force acting on a climbing GBD by the macrodislocation is smaller

0022–2461

by a factor $(1 - 2\nu)/6$ than that acting on a GBD moving along the sliding boundary.

(3) The climbing GBDs form a pile-up to compensate for the repulsive force from the sliding GBDs. The length of this pile-up is half of the grain boundary length. Repulsive interaction force between the climbing GBDs is $(1 - 2\nu)/9$ times that between the sliding GBDs.

(4) The velocity of the climbing GBDs toward their annihilating point (half-length point of the grain boundaries) determines the emission rate of the climbing GBDs, or the angular velocity of grain-rolling; thus it is the rate-controlling factor.

(5) The force acting for GBD motion, and consequently the dislocation velocity on compressive boundaries, is smaller than that on the tensile boundaries (see later Equations 8 and 9); GBDs climbing on these boundaries tend to be rate-controlling.

The GBD interactions described above are depicted schematically in Fig. 1. The resulting superplastic deformation constitutive equation of hexagonal grains is [21]:

$$\dot{\varepsilon} = 2(1 - \nu)(2 + 3\sqrt{6} - 4\nu) \times \sin^3 2\alpha \delta D_g \Omega \sigma^2 / 3\mu b_s k T d^2 \quad (1)$$

where ν is Poisson's ratio, δ is the grain boundary thickness, D_g is the grain boundary diffusion coefficient, Ω is the atomic volume, μ is the shear modulus; d is the grain diameter, σ, k and T have their usual meanings and α is the angle between the normal direction of sliding facets and the applied tensile stress.

The variation in grain diameter, or grain boundary length means a change not only in the climbing distance of sessile GBDs on facets with normal stress, but also the GBD pile-up length on the sliding facets and thus the stress generated by it at grain boundary triple junctions. Both of these factors are critical in the above-described deformation controlling mechanism. So it can be expected that, in the case of a nonequiaxed and directionally arrayed microstructure in which the grain boundary length is different in different directions, the strain-rate response to applied stress will be both orientation- and grain-aspect-ratio-dependent.

2.2. Deformation geometry: correlation of macroscopic strain rate with GBD emission rate

For simplicity, the nonequiaxed microstructure is idealized into closely packed shuttle-shaped grains as depicted in Fig. 2. Grain boundaries are 120° from each other at triple junctions, and the lengths of the longer and shorter boundaries are $d_L/2$ and $d_S/2$, respectively. We can define $\rho = d_L/d_S$ as the grain aspect ratio that represents the extent of nonequiaxity, and the angle between the normal direction of the longer facets and the applied tension stress direction is θ.

For the three adjacent boundaries OA, OB and OC in Fig. 2, the resolved shear stress coefficient (RSSC)

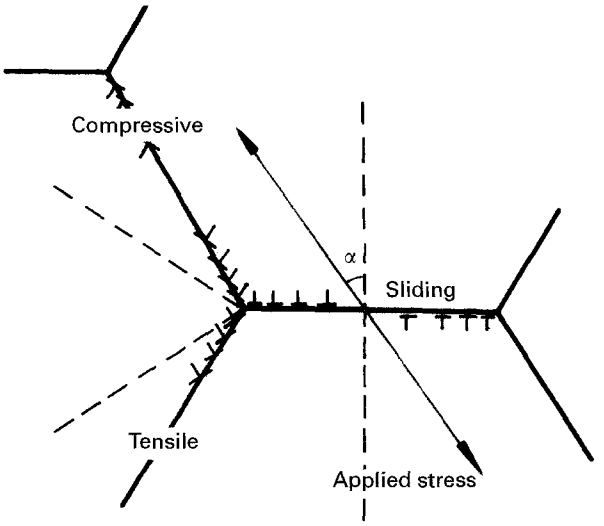

Figure 1 GBD pile-ups at triple junction.

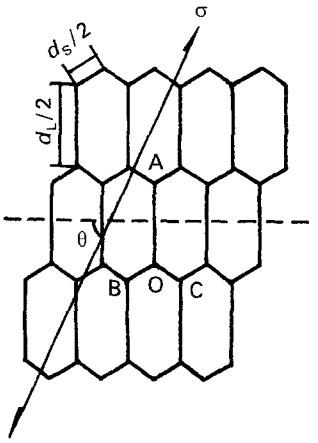

Figure 2 Model microstructure.

relationship with θ is shown in Fig. 3. The boundary with the highest RSSC, and consequently the resolved shear stress dominates its GBD movement, is expected to slide, while accommodation is carried out by the other two. The nature of the normal stress (tensile or compressive) acting upon the two sessile boundaries depends upon their relative position to the applied tensile stress (ATS); the one that lies closer to the ATS is expected to be of compressive nature and the other tensile.

We can conclude from the above that grain boundary behaviours fall into three categories with respect to the grain boundary–stress orientation relationship:

(1) $\theta = 0$–$30°$; in the three adjacent boundaries (a longer one and two shorter ones), one of the shorter ones slides, the other is compressive, the longer boundary is tensile.

(2) $\theta = 30$–$60°$; the longer one slides, the shorter ones are either tensile or compressive.

(3) $\theta = 60$–$90°$; one of the shorter ones slides, the other is tensile, and the longer one is compressive.

We shall show later that these three conditions correspond to different deformation constitutive equations.

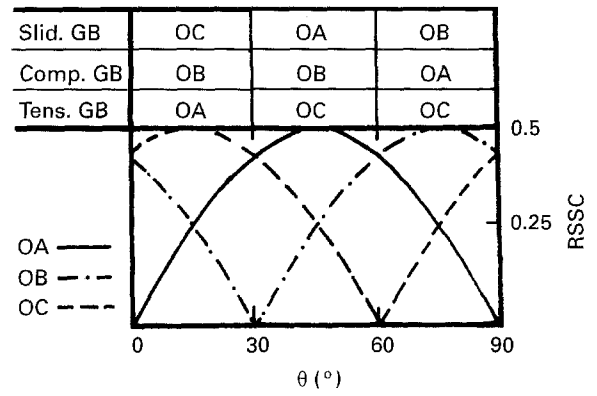

Figure 3 RSSC and stress state of grain boundaries.

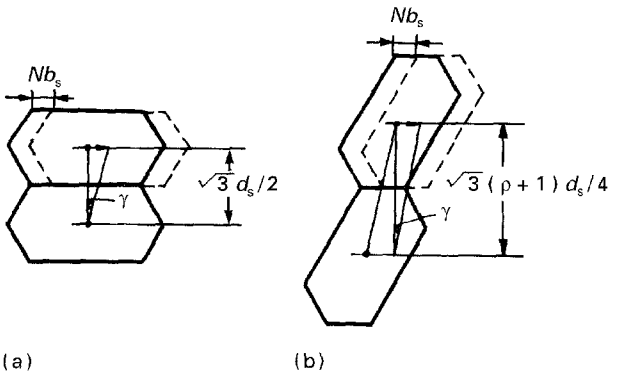

Figure 4 Shearing carried out by GBS. (a) Longer boundary sliding, (b) shorter boundary sliding.

The macroscopic strain carried out by grain boundary sliding can be correlated with the emission rate of GBDs using the simple geometry as shown in Fig. 4. When N dislocations with Burgers vector b_s glide out of the sliding facet, the slip distance of the grain boundary is Nb_s; thus the shear strains when the longer and shorter boundary slides are

$$\gamma = 2Nb_s/\sqrt{3}d_S \tag{2}$$

and

$$\gamma = 4Nb_s/\sqrt{3}\,(\rho+1)\,d_S \tag{3}$$

respectively.

A sliding GBD dissociates into two sessile GBDs at the triple point; each of these two sessile GBDs enters one of the adjacent boundaries with normal stress, so the emission rate of climbing GBDs n_c is equal to that of the sliding GBDs n_s. Thus the shear strain rate will be

$$\dot{\gamma} = 2n_c b_s/\sqrt{3}d_S \tag{4}$$

and

$$\dot{\gamma} = 4n_c b_s/\sqrt{3}\,(\rho+1)d_S \tag{5}$$

The uniaxial tensile strain rate is related to the shear strain rate by

$$\dot{\varepsilon} = \dot{\gamma}\sin\alpha\cos\alpha \tag{6}$$

where α is the angle between the normal direction of the sliding boundary and the tensile axis.

From Equations 4, 5 and 6 the relationship between macroscopic tensile strain rate and climbing GBD emission rate can be constructed.

2.3. GBD emission rate

When an uniaxial tensile stress σ is applied, the magnitude of forces acting on the GBDs arising from it are [21]

$$f_s = \sigma b_s \sin\alpha\cos\alpha \tag{7}$$

$$f_t = \sigma b_s\,[\sin\alpha\cos\alpha + (\sin^2\alpha - 1/6)]/2 \tag{8}$$

$$f_d = \sigma b_s\,[\sin\alpha\cos\alpha - (\sin^2\alpha - 1/6)]/2 \tag{9}$$

respectively, for the sliding, tensile and compressive facets.

The number of dislocations in a gliding pile-up can be stated as

$$N_s = (1-\nu)\,(d_1/2\,b_s)\,(f_s/\mu b_s)$$
$$= f_s/2\pi f_{rs}\,(L = d_1/2) \tag{10}$$

where $f_{rs} = \mu b_s/2\pi(1-\nu)\,L$, L is the average separation of GBDs in the pile-up and d_1 is twice the boundary length.

We can see that f_{rs} is equal to the repulsive force between two edge dislocations with a separation of L.

Similarly, for a nonsliding boundary with a length of $d_2/2$, where the GBD pile-up length is $d_2/4$, the number of GBDs in this pile-up to compensate the sliding macro-dislocation is

$$N_c = f_b/2\pi f_{rc}\,(L = d_2/2) \tag{11}$$

where $f_{rc} = f_{rs}(1-2\nu)/9 = (1-2\nu)\,\mu b_s/18\pi(1-\nu)L$ is the repulsive force between the climbing GBDs, f_b is the counteracting force of a climbing GBD to the sliding macrodislocation. The acting and counteracting force compensate with the equation

$$(1-2\nu)\,N_s f_s/6 = N_c f_b \tag{12}$$

From Equations 10–12 we can derive

$$f_b = (1-2\nu)\,(d_1/d_2)^{1/2} f_s/3\sqrt{6} \tag{13}$$

The climbing velocity of GBDs is [21]

$$v_c = 2\delta D_g \Omega f_c/b_c^2 KT\,(R - b_c) \tag{14}$$

where f_c is a combination of the effect of applied stress and f_b, and $R = d_2/4$ is the pile-up length.

The direct forces acting on climbing GBDs by the applied stress is expressed by Equations 8 and 9 for tensile and compressive facets, respectively. We can see from these two equations that for $\alpha = 30$–$60°$, f_t is always larger than f_d; thus the GBD climbing velocity is smaller on compressive facets, which controls the GBD emission rate at the triple point. Taking into account the fact that vacancy production is quicker on tensile facets, which accelerates the GBD annihilation process, $(f_t + f_d)/2$ can be regarded as the applied stress effect term in f_c, so

$$f_c = f_b + f_s/2 \tag{15}$$

The separation of climbing GBDs, $\overline{L_c} = d_2/4N_c$, combined with the GBD climbing velocity v_c, provides a characterization of the GBD emission rate through

$$n_c = v_c/\overline{L_c} \tag{16}$$

TABLE I Nonequiaxity effect on GBD activities

Category		I	II	III
Geometric features	θ	$0 \sim 30°$	$30 \sim 60°$	$60 \sim 90°$
	d_1	d_S	d_L	d_S
	d_2	d_S	d_S	d_L
	$\dot{\gamma} \sim n_c$	Equation 5	Equation 4	Equation 5
Parameters related to GBD activities	f_b	f_{bo}	$\rho^{1/2} f_{bo}$	$\rho^{-1/2} f_{bo}$
	f_c	$f_{bo} + f_s/2$	$f_{bo} + \rho^{1/2} f_s/2$	$f_{bo} + \rho^{-1/2} f_s/2$
	N_s	N_{so}	ρN_{so}	N_{so}
	N_c	N_{co}	$\rho^{1/2} N_{co}$	$\rho^{1/2} N_{co}$
	$\overline{L_c}$	$\overline{L_{co}}$	$\rho^{-1/2} \overline{L_{co}}$	$\rho^{1/2} \overline{L_c}$
	V_c	$A(f_{bo} + f_s/2)$	$A(f_{bo} + \rho^{1/2} f_s/2)$	$A(f_{bo} + \rho^{-1/2} f_s/2)$

The above equations will lead to the final determination of the deformation strain-rate $\dot{\varepsilon}$.

2.4. Constitutive equations

Microstructure nonequiaxity results in anisotropy of a series of critical parameters, as summarized in Table I, for the three categories derived in Section 2.2.

$$f_{bo} = f_s(1 - 2\nu)/3\sqrt{6},$$

$$N_{so} = (1 - \nu) f_s d_S/2\,\mu b_s^2$$

$$N_{co} = \sqrt{6} N_{so}/2,$$

$$\overline{L_{co}} = \mu b_s^2/\sqrt{6}\,(1 - \nu) f_s$$

correspond to the f_b, N_s, N_c and $\overline{L_c}$ values for an equiaxed microstructure with grain diameter d_S, and $A = 24\delta D_g \Omega / b_s^2 kT d_S$.

From Table I, the nonequiaxity effect on GBD activities can be clearly understood. When the longer axis of grains lies approximately perpendicular to tensile stress ($\theta = 0$–$30°$) which is the case for category I, GBD activities account for both grain boundary sliding and its correspondent controlling process taking place on shorter boundaries, GBD separation and climbing velocity, and consequently the GBD emission rate, show no difference from an equiaxed microstructure with grain size d_S. This tells us that any grain shape influence on the constitutive equations results from the deformation geometry shown in Fig. 4 and Equation 5.

As for category II ($\theta = 30$–$60°$), the longer boundary is activated for sliding and the longer length of the sliding pile-up results in a higher acting force for sessile GBD climbing. Sessile GBD separation is decreased and the climbing velocity increased. This causes a higher GBD emission rate and hence a higher strain rate for a given stress.

In the case of category III ($\theta = 60$–$90°$), the longer climbing GBD pile-up and the larger number of GBDs in it result in a higher separation of GBDs and a lower climbing velocity. These, combined with the deformation geometry effect (Equation 5), reduce the superplastic strain rate at constant stress or give a higher flow stress at a given strain rate.

According to Equations 4–6, 16 and Table I, the constitutive equations for the three categories are as follows:

Category I

$$\dot{\varepsilon} = \frac{2\delta D_g \Omega [3\sqrt{6} + 2 - 4\nu]\ (1 - \nu)\sigma^2 \sin^3 2(\theta + 30°)}{\sqrt{3}(\rho + 1)\mu b_s kT d_S^2} \tag{17}$$

Category II

$$\dot{\varepsilon} = \frac{\delta D_g \Omega [3\sqrt{6}\ \rho^{1/2} + \rho(2 - 4\nu)]\ (1 - \nu)\sigma^2 \sin^3 2\theta}{\sqrt{3}\mu b_s kT d_S^2} \tag{18}$$

Category III

$$\dot{\varepsilon} = \frac{2\delta D_g \Omega [3\sqrt{6}\,\rho^{1/2} + 2 - 4\nu]\,(1 - \nu)\,\sigma^2 \sin^3 2(\theta - 30°)}{\sqrt{3}\,\rho^2 (\rho + 1)\mu b_s kT d_S^2} \tag{19}$$

It should be pointed out that the above derivation is based on the concept that the GBD emission rate on compressive boundaries determines the deformation rate; this is true in both categories II and III. But for category I, we know from Table I that an elongated sessile boundary slows down GBD emission; if such an effect dominates, GBD climbing on the longer tensile facet, rather than on the shorter compressive facet, will control the whole deformation process. Taking the actual value of f_t and f_d (Equations 8 and 9) into account in the calculation of f_c for both tensile and compressive boundaries, and using the criterion of

$$n_{ct}/n_{cd} = \rho^{3/2} f_{ct}/f_{cd} \tag{20}$$

we can get a critical value of $\rho = \rho_o(\theta)$.

If $\rho < \rho_o(\theta)$, $n_{ct}/n_{dt} > 1$, GBD climbing on the shorter compressive boundary controls, and the constitutive equation is Equation 17.

If $\rho > \rho_o(\theta)$, deformation is controlled by GBD activity on the longer tensile boundary, and the strain-rate will be

$$\dot{\varepsilon} = \frac{2\delta D_g \Omega [\rho^{1/2}(3\sqrt{6}\sin 2\theta + 6\sqrt{2}\sin^2\theta - \sqrt{2}) + \sin 2\theta(2 - 4\nu)](1 - \nu)\sigma^2 \sin^2 2(\theta + 30°)}{\sqrt{3}\rho^2(\rho + 1)\mu b_s k T d_s^2} \quad (21)$$

The strain-rate dependence on aspect ratio will be stronger in this case than where Equation 17 dominates.

3. Discussion

In dealing with superplastic deformation behaviour of nonequiaxially grained materials, the most significant problem is, in what manner and to what extent grain shape, represented quantitatively by grain aspect ratio, affects the flow stress–strain rate relationship; this is of great importance in determining optimum superplastic forming conditions. The general description of strain-rate response to stress is often stated as

$$\dot{\varepsilon} = \dot{\varepsilon}(\sigma, \bar{S}, T)$$

Here $\bar{S}$ includes all the microstructure factors, for example mean values and distribution functions of grain size, grain aspect ratio, grain orientation, etc., and in dual or multi-phase materials the morphology of all the constitutive phases. As for a homogeneous nonequiaxed microstructure, a simplified expression in the form of

$$\dot{\varepsilon} = \dot{\varepsilon}_o(\sigma, d, T)\, g_1(\rho)\, g_2(\theta)$$

is expected. Experiments devoted to determining $g_1 \propto \rho^x$ often show a negative value of x, which means $\rho > 1$ decreases the strain-rate or increases flow stress. This is how the concept "elongated grains slow down superplastic deformation" takes its form. From the deductions in this paper, we can conclude that when the longer axis of the grains lies parallel or perpendicular to the applied stress, this is actually the case.

However, when the longer axis of grains lies in an angle range around 45° with respect to the applied stress, x is positive as shown by Equation 18; this indicates that superplastic deformation can be carried out at higher strain rates, or lower stresses in this case, compared to an equiaxed microstructure. Fig. 5 shows the superplastic strain-rate dependence on grain aspect ratio ρ in different angle ranges.

Experimental investigations on the anisotropic stress–strain rate behaviour of nonequiaxially grained Ti6Al4V with banded α and β phases, at 0°, 45° and 90° to the applied stress, showed qualitative agreement with the present model [22]. The peak m-value was observed at a strain-rate as high as $(8–10) \times 10^{-4}\,s^{-1}$ for a 45° sample, which is several times higher than equiaxed Ti6Al4V usually shows [23]. An alternative mechanism based on the difference in GBD accommodation velocity in α and β phases was described in Reference 22.

The superplastic strain-rate dependence upon orientation is depicted in Fig. 6, which is calculated from Equations 17–19 when $\nu = 0.3$ for both equiaxed and nonequiaxed microstructures. A period of 30° is predicted by the Paidar and Takeuchi model for equiaxed closely packed hexagonal grains; this is due to the periodical anisotropic nature of the model microstructure. For a nonequiaxed model, the operating range of the fast deforming system (in which the longer grain boundary acts as the sliding facet) is increased to $|\theta_2 - \theta_1| > 30°$, although the resolved shear-stress coefficient is lower when θ is out of the 30–60° range as shown by Fig. 3.

In practical materials, an equiaxed microstructure is isotropic in its deformation behaviour; a constitutive equation free of the α term results by normalization of Equation 1 to account for such a circumstance. The same treatment should be carried out for Equations 17–19. A schematic depiction is given at the upper-right corners of Fig. 6a and b, which shows the highest deformation rate and lowest flow stress at $\theta = 45°$ for an elongated microstructure, while for equiaxed grains both $\dot{\varepsilon}$–θ and σ–θ behaviours are constant.

Further complexity is likely to be brought about by applying the above consideration to the examination of superplasticity of engineering materials. It is well known that a large scatter in ρ and θ exists from position to position [24], which makes quantitative metallographic determination of the microstructure a laborious, or almost impossible, job to do. Incidentally, since a nonequiaxed microstructure is thermodynamically unstable under the condition of superplastic deformation, an equiaxiallization process, whose kinetics are rather poorly investigated [24, 25], is inevitable and must be taken into account.

Grain boundary sliding (GBS), as a deformation mechanism, is expected to occur in a wider strain-rate range in an arbitrarily oriented nonequiaxed microstructure than in a homogeneous equiaxed one, although it should be restricted to certain regions in the material; this is a reasonable prediction of the present model. The transition from GBS to dislocation creep (DC) is significantly varied in different

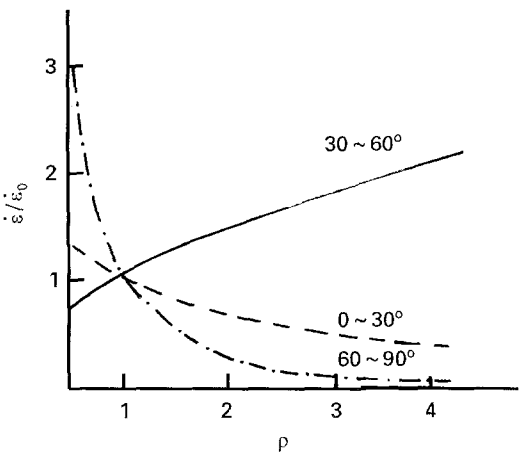

Figure 5 Superplastic deformation strain-rate dependence on grain aspect ratio.

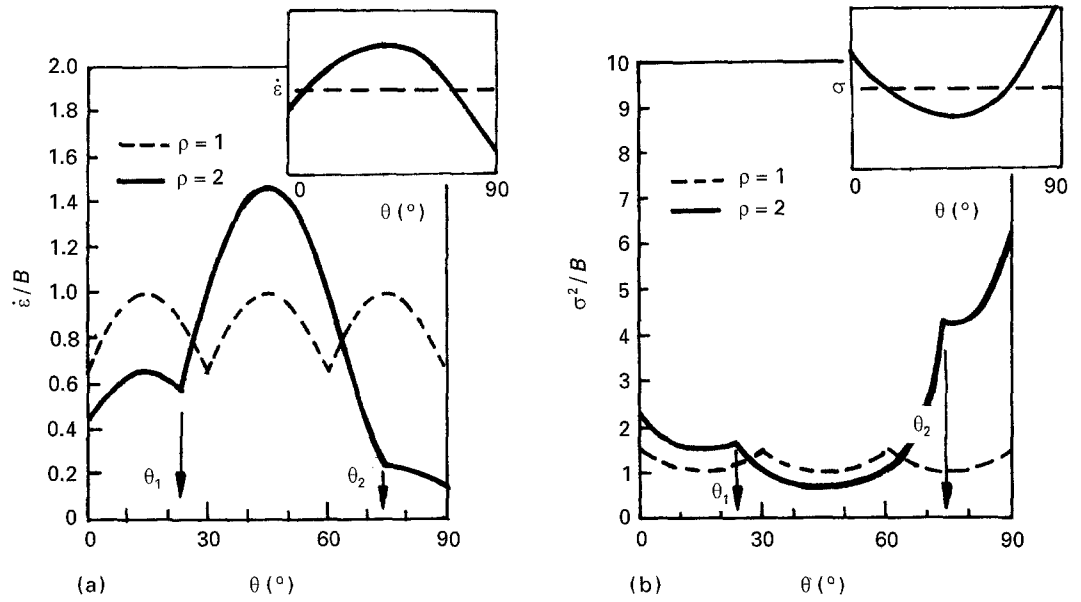

Figure 6 Deformation anisotropy caused by grain nonequiaxity. (a) Strain-rate at constant stress, (b) stress at constant strain-rate. $B = 3.3\delta D_g \Omega/\mu b_s kT d_S^2$.

regions; consequently, deformation by GBS and DC tends to coexist, and a moderate strain-rate sensitivity index m is likely to be exhibited in the overall strain-rate range. A similar effect has been well discussed in the literature on microstructure with a grain size distribution [26, 27].

Exaggerated inhomogenity caused by differently oriented nonequiaxed grains is surely detrimental to plasticity and surface quality of the deformed workpiece. However, this can be improved to some extent by accelerating the dynamic equalization and homogenization process with optimized superplastic deformation technology [28].

4. Conclusion

An analysis is made of the problem of superplastic deformation anisotropy initiated by a directionally arrayed nonequiaxed microstructure. Grain boundary sliding (GBS) is accommodated by climbing and annihilating processes of grain boundary dislocations (GBDs). Dynamics of GBD activity, combined with deformation geometry, exhibit a profound influence of grain shape on stress–strain rate relationships. Constitutive equations show a negative power dependence of strain rate on the grain aspect ratio when tensile stress is applied parallel or perpendicular to the longer axis of grains, which means elongated microstructures reduce superplastic deformation. While the applied stress lies in an angle around 45° to the longer axis, the power of strain-rate dependence on grain aspect ratio is positive, and superplastic deformation can be accelerated to some extent by a nonequiaxed microstructure.

Acknowledgements

Thanks are due to the National Natural Science Foundation of China for funding the present research. Professor V. Paidar of the Czechoslovak Academy of Sciences is also thanked for providing copies of his work, which were very helpful to the authors.

References

1. K. A. PADMANABHAN and G. L. DAVIES, in "Superplasticity" (Springer-Verlag, New York, 1980).
2. O. D. SHERBY and J. WADSWORTH, in Proceedings of the Conference on Deformation Processing and Microstructure, edited by G. Krauss (American Society for Metals, Ohio, 1984) p. 355.
3. R. C. GIFKINS, Proceedings of the Conference on Superplastic Forming of Structural Alloys, edited by N.E. Paton and C.H. Hamilton (TMS–AIME, Warrendale, 1982) p. 3.
4. J. A. WERT, *ibid.*, p. 69.
5. M. SUERY and B. BAUDELET, *J. Mater. Sci.* **10** (1975) 22.
6. C. HOMER, J. P. LECHTEN and B. BAUDELET, *Metall. Trans.* **A8** (1977) 1191.
7. W. D. NIX, *Metals Forum* **4** (1981) 38.
8. M. J. LUTON, Proceedings of the Conference on Strength of Metals and Alloys, Vol. 2, edited by H.J. Mcqueen *et al.* (Pergamon Press, Montreal, 1985) p. 859.
9. C. D. INGELBRECHT and P. G. PATRIDGE, *J. Mater. Sci.* **21** (1986) 4071.
10. A. BALL and M. M. HUTCHISON, *Met. Sci. J.* **3** (1969) 1.
11. A. K. MUKHERJEE, *Mater. Sci. Engng* **8** (1971) 83.
12. M. F. ASHBY and R. A. VERRALL, *Acta Metall.* **21** (1973) 149.
13. R. C. GIFKINS, *Metall. Trans.* **A7** (1976) 1225.
14. J. H. GITTUS, Trans. ASME, *J. Engng Mater. Technol.* **99** (1977) 244.
15. A. ARIELI and A. K. MUKHERJEE, *Mater. Sci. Engng* **45** (1980) 61.
16. A. K. GHOSH and R. RAJ, *Acta Metall.* **29** (1981) 607.
17. A. E. GECKINLI, *Met. Sci.* **17** (1983) 12.
18. O. A. KAIBYSHEV, R. Z. VALIEV and A. K. EMALTDINOV, *Phys. Stat. Sol.* (*a*) **90** (1985) 197.
19. J. Z. CUI and L. X. MA, *Acta Metall. Sin.* **24** (4) (1988) B288.
20. A. K. GHOSH and C.-H. CHENG, Proceedings of the Conference on Superplasticity in Advanced Materials, edited by S. Hori, M. Tokizane and N. Furushiro, 3–6 June, 1991, Osaka, Japan, p. 299.
21. V. PAIDAR and S. TAKEUCHI, *Acta Metall. Mater.* **40** (1992) 1773.
22. J. L. WAN, J.L. GU and N.P. CHEN, Proceedings of the 8th National Symposium on Titanium and Titanium Alloys, China, 1993, p. 410.

23. N. E. PATON and C. H. HAMILTON, *Metall. Trans.* **A10** (1979) 241.
24. O. A. KAIBYSHEV, R. Y. LUTFULLIN and G. A. SALISHCHEV, *Fiz. Metal. Metalloved.* **66** (1988) 966.
25. O. A. KAIBYSHEV, R.Y. LUTFULLIN and G.A. SALISHCHEV, *ibid.* **66** (1988) 1163.
26. R. RAJ and A. K. GHOSH, *Acta Metall.* **29** (1981) 607.
27. LONGQUAN SHI and D. O. NORTHWOOD, *Acta Metall. Mater.* **40** (1992) 2069.
28. B. Z. BAI, PhD thesis, Tsinghua University, Beijing (1990).

Received 15 June 1994
and accepted 21 February 1995